

# Synthesis and Characterization of Side-Chain Cholesteric Liquid-Crystalline Polymers Derived from Steroid Substituents

Jian-She Hu, Bao-Yan Zhang, Wei Pan, Yuan-Hao Li, Shi-Chao Ren

Center for Molecular Science and Engineering, Northeastern University, Shenyang, People's Republic of China

Received 22 January 2005; accepted 19 May 2005

DOI 10.1002/app.22700

Published online 14 December 2005 in Wiley InterScience (www.interscience.wiley.com).

**ABSTRACT:** A series of new cholesteric liquid-crystalline polysiloxanes derived from steroid substituents were synthesized. The chemical structures of the monomers or polymers obtained were characterized by FTIR, element analyses,  $^1\text{H}$  NMR, and  $^{13}\text{C}$  NMR. Their mesogenic properties and thermal stability were investigated by differential scanning calorimetry, thermogravimetric analysis, polarizing optical microscopy, and X-ray diffraction measurements. Mono-

mers exhibited typical cholesteric focal-conic or spiral texture. The polymers  $\text{P}_1$ – $\text{P}_6$  showed cholesteric phase and  $\text{P}_7$  displayed smectic phase. © 2005 Wiley Periodicals, Inc. *J Appl Polym Sci* 99: 2330–2336, 2006

**Key words:** liquid-crystalline polymers; synthesis; cholesteric phase; steroid groups

## INTRODUCTION

In recent years, considerable interest has centered on cholesteric liquid-crystalline polymers (LCPs), mainly because of their unique optical properties, including selective reflection of light, thermochromism, and circular dichroism, and potential applications such as nonlinear optical devices, full-color thermal imaging, and specific organic pigment.<sup>1–9</sup> The cholesteric phase is formed by rodlike, chiral molecules responsible for macroscopical alignment of cholesteric domains. Depending on chemical structures, it may be feasible to achieve a macroscopic alignment of cholesteric domains. For comblike polymers, the mesogenic properties of side-chain LCPs mainly depend on the nature of polymer backbone, the type of the mesogen, the length of the flexible spacer, and the nature of terminal groups.<sup>10–13</sup> The polymer backbones of side-chain LCPs are primarily polyacrylates, polymethacrylates, and polysiloxanes; however, polyacrylates and polymethacrylates, because of their backbones, show higher glass transition temperatures ( $T_g$ ) and higher viscosity. For higher mobility of the mesophase and

mesogenic properties at moderate temperature, the polysiloxanes' backbone and the flexible spacer are usually adopted. Recently, many novel cholesteric LC materials have been reported.<sup>14–22</sup> Therefore, it would be necessary to synthesize various kinds of new cholesteric LCPs to explore their potential applications.

In this study, a series of cholesteric LCPs derived from cholesteryl 4-(10-undecylen-1-yloxy)benzoate ( $\text{M}_1$ ) and diosgeninyl 4-allyloxybenzoate ( $\text{M}_2$ ) were synthesized and characterized. The mesomorphic properties and thermal stability of the monomers and polymers obtained were investigated with differential scanning calorimetry (DSC), thermogravimetric analysis (TGA), polarizing optical microscopy (POM), and X-ray diffraction (XRD).

## EXPERIMENTAL

### Materials

Polymethylhydrosiloxane (PMHS,  $\bar{M}_n = 700$ –800) was purchased from Jilin Chemical Industry (Jilin, China). Cholesterol was purchased from Henan Xiayi Medical (Zhoukou, China). Diosgenin was purchased from Wuhan Ruixin Chemical (Wuhan, China).  $\text{H}_2\text{PtCl}_6$  catalyst was obtained from Shenyang Chemical Reagent. All solvents and reagents were purified by standard methods.

### Characterization

FTIR spectra were measured on a Perkin–Elmer spectrum One (B) spectrometer (Perkin–Elmer, Foster City,

Correspondence to: B.-Y. Zhang (baoyanzhang@hotmail.com or byzcong@163.com).

Contract grant sponsors: National Natural Science Fundamental Committee of China; HI-Tech Research and Development Program (863) of China; China Postdoctoral Science Foundation; and Science and Technology Bureau of Shenyang.

CA). The element analyses (EA) were carried out by using a Elementar Vario EL III (Elementar, Germany).  $^1\text{H}$  NMR spectra (300 MHz) and  $^{13}\text{C}$  NMR (75.4 MHz) spectra were obtained with a Varian Gemini 300 spectrometer (Varian Associates, Palo Alto, CA). Optical rotations were obtained on a Perkin-Elmer 341 polarimeter. Phase transition temperatures and thermodynamic parameters were determined by using a Netzsch DSC 204 (Netzsch, Wittelsbacherstr, Germany) equipped with a liquid nitrogen cooling system. The heating and cooling rates were  $10^\circ\text{C}/\text{min}$ . The thermal stability of the polymers under atmosphere was measured with a Netzsch TGA 209C thermogravimetric analyzer. A Leica DMRX (Leica, Wetzlar, Germany) POM equipped with a Linkam THMSE-600 (Linkam, Surrey, England) hot stage was used to observe phase transition temperatures and analyze LC properties for the monomers and polymers through observation of optical textures. XRD measurements were performed with a nickel-filtered  $\text{Cu-K}\alpha$  radiation with a DMAX-3A Rigaku (Rigaku, Tokyo, Japan) powder diffractometer.

### Synthesis of the monomers

The synthetic route to the olefinic monomers is shown in Scheme 1.

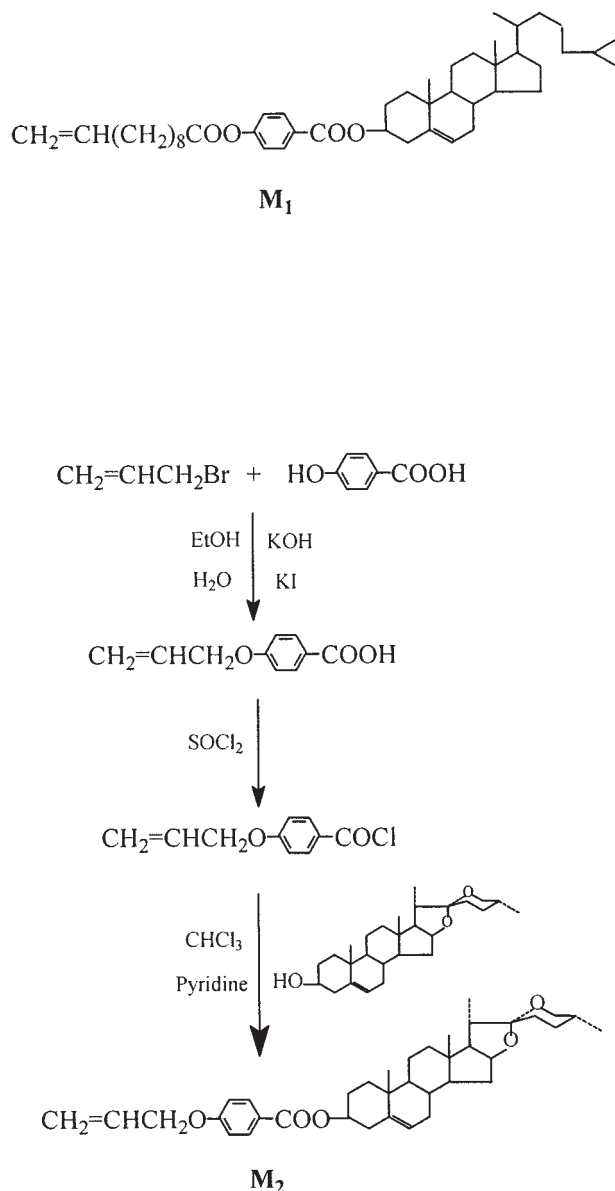
#### Cholesteryl 4-(10-undecylen-1-yloxy)benzoate ( $\mathbf{m}_1$ )

$\mathbf{M}_1$  was prepared according to the procedures previously reported.<sup>23</sup> Yield 46%, m.p.  $110^\circ\text{C}$ ;  $[\alpha]_D^{28} -4.7^\circ$  ( $c = 0.703$ , toluene).

IR (KBr,  $\text{cm}^{-1}$ ): 3064 ( $=\text{C}-\text{H}$ ); 2930, 2852 ( $-\text{CH}_3$ ,  $-\text{CH}_2-$ ); 1767, 1716 ( $\text{C}=\text{O}$ ); 1635 ( $\text{C}=\text{C}$ ); 1603, 1504 (Ar). Elem. Anal. Calcd. for  $\text{C}_{45}\text{H}_{68}\text{O}_4$ : C, 80.31%; H, 10.18%. Found: C, 80.23%; H, 10.39%.  $^1\text{H}$  NMR ( $\text{CDCl}_3$ , TMS)  $\delta$  ppm: 0.61–2.72 [m, 59H,  $-(\text{CH}_2)_8-$  and cholesteryl- $\text{H}$ ]; 4.25 (t, 1H,  $-\text{ArCOOCH}<$ ); 5.10 (m, 2H,  $\text{CH}_2=\text{CH}-$ ); 5.50 (d, 1H,  $=\text{CH}-$  in cholesteryl), 6.08 (m, 1H,  $=\text{CH}-$ ), 7.05–8.15 (m, 4H, Ar- $\text{H}$ ).  $^{13}\text{C}$  NMR ( $\text{CDCl}_3$ , TMS)  $\delta$  ppm: 18.6, 19.8, 21.8 (methyl- $\text{C}$ ); 20.6, 21.7, 22.3, 24.9, 25.0, 29.5, 29.7, 30.0, 30.3, 31.9, 32.3, 32.5, 33.7, 34.2, 36.3, 40.1, 40.4 (methylene- $\text{C}$ ); 28.2, 30.1 (aliphatic tertiary C); 112.2, 129.8 (aromatic tertiary C); 29.2, 43.3, 46.8, 47.9, 74.9 (tertiary C in cholesteryl); 126.5, 157.8 (aromatic quaternary C); 39.6, 41.2 (quaternary C in cholesteryl); 113.8 ( $\text{CH}_2=$ ); 140.9 ( $=\text{CH}-$ ); 122.2 ( $=\text{CH}-$  in cholesteryl); 149.5 ( $>\text{C}=\text{O}$  in cholesteryl); 166.7, 169.2 ( $\text{C}=\text{O}$ ).

#### Diosgeninyl 4-allyloxybenzoate ( $\mathbf{m}_2$ )

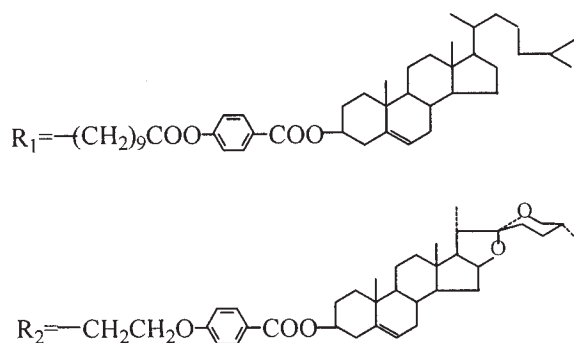
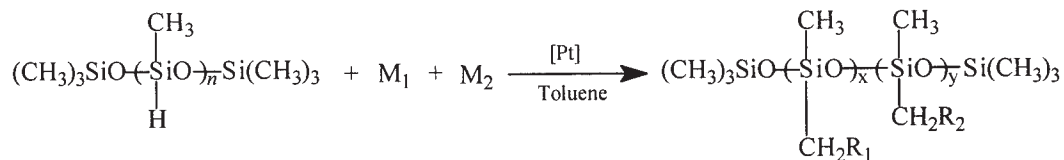
4-Allyloxybenzoyl chloride (19.6 g, 0.1 mol) was added dropwise to a cold solution of diosgenin (41.4 g, 0.1 mol) in chloroform (150 mL) and pyridine (8 mL).



Scheme 1 Synthesis of LC monomers.

The reaction mixture was refluxed for 15 h. The crude product was obtained by adding ethanol to filtrate, and recrystallized from acetic ether. White crystals were obtained. Yield 66%; mp  $182^\circ\text{C}$ ;  $[\alpha]_D^{28} -43.5^\circ$  ( $c = 0.774$ , toluene).

IR (KBr,  $\text{cm}^{-1}$ ): 3074 ( $=\text{C}-\text{H}$ ); 2944, 2830 ( $-\text{CH}_3$ ,  $-\text{CH}_2-$ ); 1713 ( $\text{C}=\text{O}$ ); 1643 ( $\text{C}=\text{C}$ ); 1606, 1455 (Ar); 1249 ( $\text{C}-\text{O}-\text{C}$ ). Elem. Anal. Calcd. for  $\text{C}_{37}\text{H}_{50}\text{O}_5$ : C, 77.31%; H, 8.77%. Found: C, 77.15%; H, 8.91%.  $^1\text{H}$  NMR ( $\text{CDCl}_3$ , TMS)  $\delta$  ppm: 0.78–2.46 [m, 36H, diosgeninyl- $\text{H}$ ]; 3.34–3.52 (t, 3H,  $>\text{CHO}-$  and  $-\text{OCH}_2-$  in diosgeninyl); 4.38–4.81 (t, 3H,  $-\text{ArCOOCH}<$ ,  $-\text{CH}_2\text{OAr}-$ ); 5.26 (m, 2H,  $\text{CH}_2=\text{CH}-$ ); 5.39 (m, 1H,  $=\text{CH}-$  in diosgeninyl), 6.04 (m, 1H,  $=\text{CH}-$ ), 6.91–7.99 (m, 4H, Ar- $\text{H}$ ).  $^{13}\text{C}$  NMR ( $\text{CDCl}_3$ , TMS)  $\delta$  ppm: 6.1, 16.5, 20.8, 21.3 (methyl- $\text{C}$ ); 21.5,



Scheme 2 Synthesis of LC polysiloxanes.

24.3, 26.7, 30.5, 31.7, 32.0, 32.5, 32.7, 39.6, 69.1, 75.4 (methylene—C); 30.1, 30.2, 36.4, 40.5, 42.3, 47.5, 68.6, 76.1 (tertiary C in diosgeninyl); 113.6, 131.1 (aromatic tertiary C); 35.5, 39.8, 111.9 (quaternary C in diosgeninyl); 123.2, 165.3 (aromatic quaternary C); 116.3 (CH<sub>2</sub>=); 138.2 (=CH—); 121.9 (=CH— in diosgeninyl); 148.5 (>C= in diosgeninyl); 168.4 (C=O).

### Synthesis of the polymers

The synthesis of the polymers **P**<sub>1</sub>–**P**<sub>7</sub> is shown in Scheme 2. **P**<sub>1</sub>–**P**<sub>7</sub> were synthesized by same methods. For the synthesis of **P**<sub>3</sub>, the monomers **M**<sub>1</sub>, **M**<sub>2</sub>, and PMHS (Table I) were dissolved in toluene. The reaction mixture was heated to 65°C under nitrogen, and then 2 mL of THF solution of H<sub>2</sub>PtCl<sub>6</sub> catalyst (5 mg/mL) was injected with a syringe. The hydrosily-

lation reaction, monitored from the Si—H stretch intensity, was completed within 30 h, as indicated by IR. The polymers were obtained and purified by several reprecipitation from toluene solution into methanol, and then dried in vacuum.

IR (KBr): 2949–2869 (—CH<sub>3</sub>, —CH<sub>2</sub>—); 1766, 1715 (C=O); 1608, 1505 (Ar); 1300–1000 cm<sup>-1</sup> (Si—O—Si, C—Si and C—O—C).

## RESULTS AND DISCUSSION

### Synthesis

The target monomers and polymers were synthesized in accordance with Schemes 1 and 2. **M**<sub>1</sub> was prepared according to the literature procedures reported by Hu et al.<sup>23</sup> **M**<sub>2</sub> was obtained through 4-allyloxybenzoyl chloride reacted with diosgenin in chloroform in present of pyridine. Structures of **M**<sub>1</sub> and **M**<sub>2</sub> were characterized by IR, <sup>1</sup>H NMR, and <sup>13</sup>C NMR spectrum. Figure 1 shows the <sup>1</sup>H NMR spectra of **M**<sub>2</sub> in CDCl<sub>3</sub>. IR spectra of **M**<sub>2</sub> confirmed the presence of characteristic bands at 1713, 1606, and 1455 cm<sup>-1</sup> attributed to ester C=O and aromatic stretching band. <sup>1</sup>H NMR spectra of **M**<sub>2</sub> showed multiplet at 6.91–7.99, 5.26–6.04, and 0.78–3.52 ppm corresponding to aromatic protons, olefinic protons, and methyl and methylene protons, respectively.

The polymers were prepared by hydrosilylation reaction. IR spectra of the polymers showed the complete disappearance of Si—H stretching band at 2166 cm<sup>-1</sup>. Characteristic Si—O—Si stretching bands appeared at 1300–1000 cm<sup>-1</sup>. In addition, the absorption

TABLE I  
Polymerization and Solubility

Polymer	Feed (mmol)		M <sub>2</sub> <sup>a</sup> (mol %)	Yield (%)	Solubility <sup>b</sup>	
	M <sub>1</sub>	M <sub>2</sub>			Toluene	THF
P <sub>1</sub>	7.00	0.00	0	91	+	(+)
P <sub>2</sub>	6.00	1.00	14.3	89	+	(+)
P <sub>3</sub>	5.00	2.00	28.6	90	+	(+)
P <sub>4</sub>	4.00	3.00	42.9	88	+	(+)
P <sub>5</sub>	3.00	4.00	57.1	89	+	(+)
P <sub>6</sub>	2.00	5.00	71.4	91	+	(+)
P <sub>7</sub>	0.00	7.00	100	93	+	(+)

<sup>a</sup> Molar fraction of **M**<sub>2</sub> based on (**M**<sub>1</sub> + **M**<sub>2</sub>).

<sup>b</sup> +, soluble; (+), little soluble.

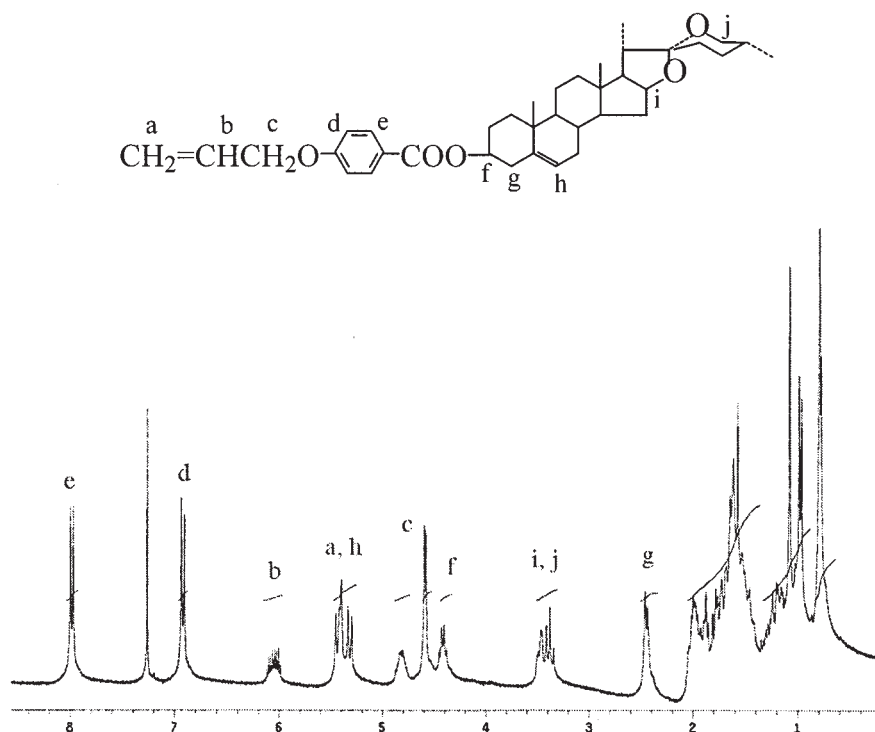


Figure 1  $^1\text{H}$  NMR spectra of  $\text{M}_2$ .

bands of ester  $\text{C}=\text{O}$  and aromatic still existed. The polymerization, yields, and solubility of the polymers are summarized in Table I. All polymers were powder, and were soluble in toluene and xylene, but were less soluble in tetrahydrofuran, chloroform, and *N,N*-dimethylformamide.

### Thermal properties

The phase transition temperatures and corresponding enthalpy changes of monomers  $\text{M}_1$ ,  $\text{M}_2$ , and polymers  $\text{P}_1$ – $\text{P}_7$ , obtained on the second heating and the first cooling scan, are summarized in Tables II and III. All phase transitions were reversible and did not change on repeated heating and cooling cycles. The phase transition temperatures determined by DSC were consistent with POM observation results.

DSC curves of  $\text{M}_1$  have been shown in the reported literature.<sup>23</sup> DSC heating thermogram of  $\text{M}_2$  contained two endotherms of the phase, which represented a melting transition at 182.3°C and a cholesteric–isotropic phase transition at 207.6°C. On cooling scans of  $\text{M}_2$ , an isotropic–cholesteric phase transition appeared at 205.4°C and crystallization appeared at 158.9°C.

DSC thermogram of  $\text{P}_1$ – $\text{P}_7$  displayed a glass transition at low temperature and a LC–isotropic phase transition at high temperature. Figure 2 shows the influence of the copolymer composition on the phase behavior of the polymers. With increasing the

concentration of  $\text{M}_2$  units,  $T_g$  of  $\text{P}_1$ – $\text{P}_7$  increased, and the clearing temperature ( $T_i$ ) first increased, then decreased, and finally increased again. It is well-known that  $T_g$  is an important parameter in connection with structures and properties. For side-chain LCPs,  $T_g$  is influenced by the nature of the polymer backbone, the rigidity of the mesogenic groups, the length of the

TABLE II  
Phase Transition Temperatures of Monomers

Monomers	Transition temperature <sup>a</sup> (°C)	Corresponding enthalpy changes (J/g)	
$\text{M}_1$	Heating	K 110.0	20.6
		Ch 195.5	1.8
		I	-
	Cooling	I 185.5	0.5
		Ch 69.4	19.2
		K	-
$\text{M}_2$	Heating	K 182.3	36.5
		Ch 207.6	1.2
		I	-
	Cooling	I 205.4	2.6
		Ch 158.9	29.7
		K	-

<sup>a</sup> K, solid; Ch, cholesteric; and I, isotropic.

TABLE III  
LC Properties of Polymers

Polymer	$T_g$ (°C)	$T_i$ (°C)	$\Delta T^a$	$T_d^b$ (°C)	LC phase
P <sub>1</sub>	38.6	233.6	195.0	316.2	Ch
P <sub>2</sub>	44.0	248.2	204.2	314.1	Ch
P <sub>3</sub>	51.2	259.5	208.3	320.0	Ch
P <sub>4</sub>	55.9	240.1	184.2	312.1	Ch
P <sub>5</sub>	67.5	233.4	165.9	323.8	Ch
P <sub>6</sub>	75.7	255.3	179.6	319.2	Ch
P <sub>7</sub>	118.4	300.7	182.3	330.8	S <sub>A</sub>

Ch, cholesteric; S, smectic.

<sup>a</sup> Mesophase temperature ranges ( $T_i - T_g$ ).

<sup>b</sup> Temperature at which 5% weight loss occurred.

flexible spacer, and the copolymer composition. In general, bulky side groups impose additional constraints on the motion of chain segments because of the steric hindrance effect and cause an increase in the  $T_g$ . However,  $T_g$  is also affected by the length of the flexible spacer of side groups similar to the plasticization effect. As shown in Table III,  $T_g$  increased from 38.6°C of P<sub>1</sub> to 118.4°C of P<sub>7</sub> when the concentration of M<sub>2</sub> increased from 0 to 100 mol % for the following reasons: (1) the plasticization effect of the flexible spacer of side groups decreased and (2) the concentration of bulky steroid groups increased.

The thermal stability of polymers is usually detected with TGA. The carbon, hydrogen, and oxygen atom in the polymers have been completely combusted when heated to 600°C. TGA results of the polymers are shown in Table III. TGA results showed that the temperatures at which 5% weight loss occurred ( $T_d$ ) were greater than 310°C for P<sub>1</sub>–P<sub>7</sub>, and this

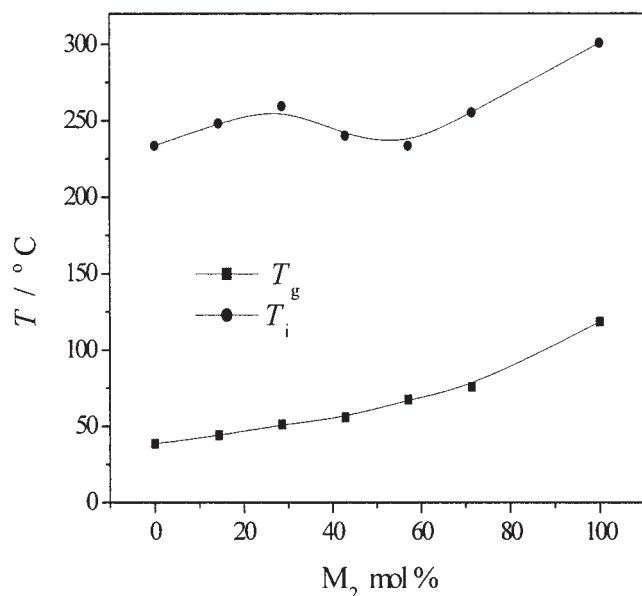
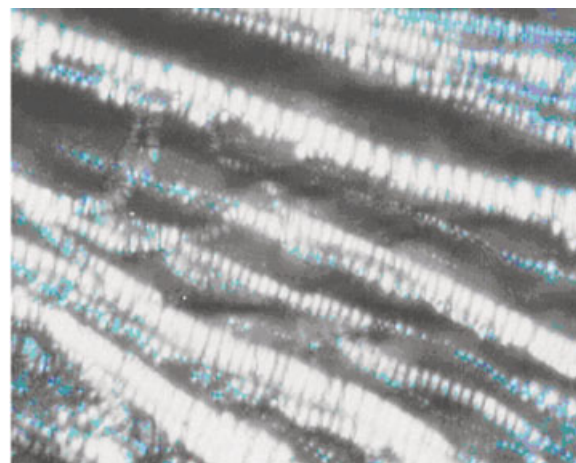
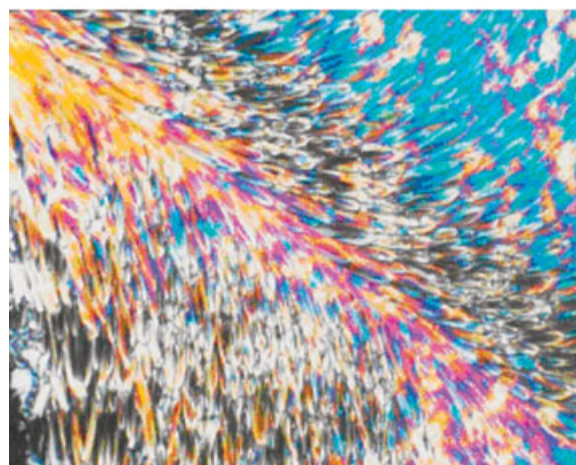


Figure 2 Effect of M<sub>2</sub> concentration on the phase transition temperatures of the polymers.



(a)



(b)

Figure 3 Optical textures of monomers ( $\times 200$ ): (a) oily-streak texture of M<sub>2</sub> on heating to 206.1°C; and (b) focal-conic of M<sub>2</sub> on cooling to 176.3°C. [Color figure can be viewed in the online issue, which is available at [www.interscience.wiley.com](http://www.interscience.wiley.com).]

demonstrates that the synthesized polymers have a high thermal stability.

### Texture analysis

In general, cholesteric LC at zero field exhibits two optically contrasting stable states: planar (including oily-streak and Grandjean) texture and focal-conic texture, when cholesteric phase is in the planar texture, the helical axis is perpendicular to the cell surface, and the material Bragg-reflects colored light; when cholesteric phase is in the focal-conic texture, the helical axis is more or less parallel to the cell surface, the material is forward-scattering, and does not exhibit selective light reflection.

The optical textures of the LC monomers and polymers are observed by POM with hot stage under

nitrogen atmosphere. POM results showed that  $M_1$  and  $M_2$  showed enantiotropic cholesteric phase on heating and cooling cycles. Optical textures of  $M_1$  have been shown in the reported literature.<sup>23</sup> When  $M_2$  was heated to 182°C, the oily-streak texture appeared, and the texture disappeared at 210°C. Cooling isotropic state, the focal-conic texture appeared at 209°C, if a slight shearing was superimposed on the melt, the focal-conic texture transformed into the oily-streak texture and the selective reflection occurred, and crystallized at 149°C. Optical textures of  $M_2$  are shown in Figure 3(a) and 3(b).

The polymer  $P_7$  showed the smectic fan-shaped texture, and the expected cholesteric texture did not occur, the reason is that the polymeric chains hinder the formation of helical supermolecular structure of the mesogens and the mesogenic moieties are ordered in a smectic orientation with their centers of gravity in planes. In general, LCPs containing chiral and nematic units can induce cholesteric phase. However, previous report<sup>24,25</sup> showed the LCPs containing mesogenic units with longer flexible spacer can also produce cholesteric phase because the cholesteric units can be freely moved by introducing longer enough units with flexible segments. The copolymers  $P_1$ – $P_6$  exhibited cholesteric Grandjean texture, and this indicates that the introduction of the mesogenic units and longer units with flexible segments into the LCPs can also produce the cholesteric phase. Photomicrograph of  $P_3$  as an example is shown in Figure 4.

### XRD analysis

In general, a sharp and strong peak at low angle ( $1^\circ < 2\theta < 4^\circ$ ) in small angle X-ray scattering (SAXS) curves and a strong broad peak associated with lateral packing at  $2\theta = 20^\circ$  or so can be observed in wide angle

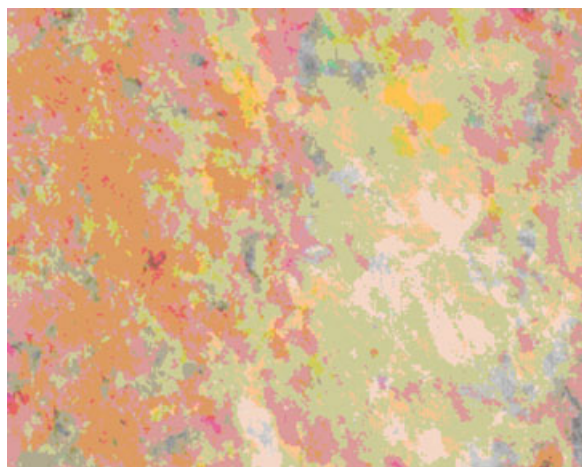


**Figure 4** Optical textures of  $P_3$  at 227.9°C ( $\times 200$ ). [Color figure can be viewed in the online issue, which is available at [www.interscience.wiley.com](http://www.interscience.wiley.com).]

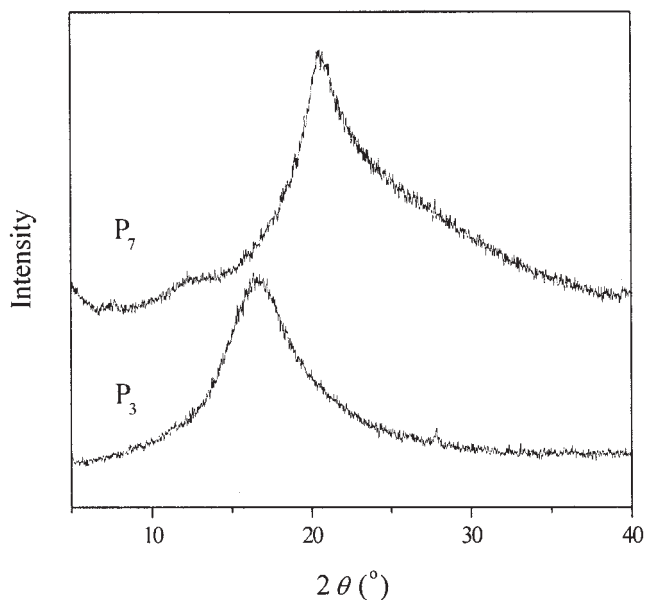


**Figure 5** XRD patterns of quenched samples.

X-ray diffraction (WAXD) curves for a smectic structure; no peak appears in SAXS curves and a broad peak occurred at  $2\theta = 16$ – $18^\circ$  or so for a cholesteric structure. Figure 5 shows representative WAXD curves of quenched samples. A strong small angle reflection associated with the smectic layers was observed at  $2\theta = 2.7^\circ$ , corresponding to  $d$ -spacing of  $d = 37.8$  and  $36.4$  Å for  $P_7$ . However, a strong small angle reflection was not observed and a broad peak appeared at  $2\theta = 16.4$ – $17.2^\circ$  for  $P_1$ – $P_6$ . Therefore, the LC phase structure was confirmed by optical textures and XRD results.

### CONCLUSIONS

In this study, two cholesteric monomers and a series of LCPs were synthesized and characterized. Monomers  $M_1$  and  $M_2$  exhibited the typical cholesteric oily-streak texture and focal-conic texture. Polymers  $P_1$ – $P_6$  showed cholesteric phase and  $P_7$  showed smectic phase. Moreover, the introduction of the mesogenic units with longer flexible segments into LCPs can induce the cholesteric phase. All of the obtained polymers exhibited wider mesophase temperature ranges and high thermal stability.

### References

1. MCDonell, D. G. In *Thermotropic Liquid Crystals*, 2nd ed.; Gray, G. W. Ed.; Wiley: New York, 1987; p 120.
2. Belayev, S. V.; Schadt, M. I.; Funfschilling, J.; Malimoneko, N. V.; Schmitt, K. *Jpn J Appl Phys* 1990, 29, L634.
3. Broer, D. J.; Lub, J.; Mol, G. N. *Nature* 1995, 378, 467.
4. Bunning, T. J.; Kreuzer, F. H. *Trends Polym Sci* 1995, 3, 318.

5. Yang, D. K.; West, J. L.; Chien, L. C.; Doane, J. W. *J Appl Phys* 1994, 76, 1331.
6. Kricheldorf, H. R.; Sun, S. J.; Chen, C. P.; Chang, T. C. *J Polym Sci Part A: Polym Chem* 1997, 35, 1611.
7. Peter, P. M. *Nature* 1998, 391, 745.
8. Sapich, B.; Stumpe, J.; Krawinkel, T.; Kricheldorf, H. R. *Macromolecules* 1998, 31, 1016.
9. Sun, S. J.; Liao, L. C.; Chang, T. C. *J Polym Sci Part A: Polym Chem* 2000, 38, 1852.
10. Le Barney, P.; Dubois, J. C.; Friedrich, C.; Noel, C. *Polym Bull* 1986, 15, 341.
11. Hsu, C. S.; Percec, V. *J Polym Sci Part A: Polym Chem* 1989, 27, 453.
12. Hsieh, C. J.; Wu, S. H.; Hsiue, G. H.; Hsu, C. S. *J Polym Sci Part A: Polym Chem* 1994, 32, 1077.
13. Wu, Y. H.; Lu, Y. H.; Hsu, C. S. *J Macromol Sci Pure Appl Chem* 1995, 32, 1471.
14. Stohr, A.; Strohhriegl, P. *Macromol Chem Phys* 1998, 199, 751.
15. Dierking, I.; Kosbar, L. L.; Held, G. A. *Liq Cryst* 1998, 24, 387.
16. Pfeuffer, T.; Strohhriegl, P. *Macromol Chem Phys* 1999, 200, 2480.
17. Espinosa, M. A.; Cadiz, V.; Galia, M. *J Polym Sci Part A: Polym Chem* 2001, 39, 2847.
18. Finkelmann, H.; Kim, S. T.; Munoz, A.; Taheri, B. *Adv Mater* 2001, 13, 1069.
19. Kim, S. T.; Finkelmann, H. *Macromol Rapid Commun* 2001, 22, 429.
20. Hu, J. S.; Zhang, B. Y.; Sun, K.; Li, Q. Y. *Liq Cryst* 2003, 30, 1267.
21. Hu, J. S.; Zhang, B. Y.; Jia, Y. G.; Chen, S. *Macromolecules* 2003, 36, 9060.
22. Zhang, B. Y.; Hu, J. S.; Jia, Y. G.; Du, B. G. *Macromol Chem Phys* 2003, 204, 2123.
23. Hu, J. S.; Zhang, B. Y.; Liu, L. M.; Meng, F. B. *J Appl Polym Sci* 2003, 90, 3944.
24. Zhang, B. Y.; Hu, J. S.; Wang, Y.; Qian, J. H. *Polym J* 2003, 35, 476.
25. Hu, J. S.; Zhang, B. Y.; Guan, Y. *J Polym Sci Part A: Polym Chem* 2004, 42, 5262.